Electronic Supplementary Material (ESI) for ChemComm.

Designed Electron-Deficient Gold Nanoparticles for Room-Temperature C_{sp3}-C_{sp3} Coupling Reaction

Qiu-Ying Yu, Hui Su, Guang-Yao Zhai, Shi-Nan Zhang, Lu-Han Sun, Jie-Sheng Chen and Xin-Hao Li*
*Correspondence authors. Email: xinhaoli@sjtu.edu.cn

School of Chemistry and Chemical Engineering, Shanghai Jiao Tong University, Shanghai 200240 (P. R. China)

1. Material

Carbon (mesoporous) and sodium borohydride were provided by Macklin. Boric acid was purchased from Aladdin. Gold (III) chloride (Au≥50%) and other chemicals were purchased from Adamas.

2. Instruments

The scanning electron microscope (SEM) images were examined by a JEOL JSM-6700F field emission scanning electron microscope. The powder X-ray diffraction (XRD) patterns were collected on a Bruker D8 Advance X-ray diffractometer equipped with Cu-Kα radiation ($\lambda = 1.5406$ Å) and tube current of 30 mA. Transmission electron microscopy (TEM) and high resolution transmission electron microscope (HRTEM) images were performed on a TALOS F200X transmission electron microscope. The nitrogen adsorption/desorption measurements were estimated on an ASAP2020 Accelerated Surface Area and Porosimetry (Micromeritics Inc., USA). The surface area of the sample was calculated by the Brunauer-Emmett-Teller (BET) method, the pore size distributions of mesopores were calculated by the Barret-Joyner-Halenda (BJH) methods. The X-ray photoelectron spectroscopy (XPS) measurements were conducted on a Thermo ESCALAB spectrometer. The UPS was examined by a Kratos Axis Ultra DLD spectrometer. The gas chromatography (GC) analysis was performed on Shimadzu GC-2014 gas chromatograph. Gas chromatography-mass spectrometry (GC-MS) analysis was taken on SHIMADZU GCMS-QO2010 SE. The content of gold and boron were determined by inductively coupled plasma (ICP) measurements on an icap7600 spectrometer. The temperature-programmed desorption (TPD) was tested using AutoChem-Discovery 2920 with a thermal conductivity detector (TCD) signal. 100 mg of sample was placed in a U-shaped quartz reactor followed by being pre-treated in He flow at 150 °C for 30 min and cooled to room temperature. The desorbed temperature of (1-bromoethyl) benzene was from 50 °C to 250 °C. Conversions of all substrates were calculated via gas chromatography or gas chromatography-mass spectrometer analysis.

3. Methods

Synthesis of BC-x: Boric acid (5.7 g, 11.4 g, 22.8 g), carbon (2 g) were mixed into 250 mL of H_2O. The mixture was stirred and dried at 70 °C. Then, the solid power was heated up to 900 °C for 2 h under N_2 gas flow. The as-obtained boron-doped carbon samples were named as BC-0.5, BC-1 and BC-2, respectively (x represents the mole ratio of B/C in the precursor).

Synthesis of Au_y/BC-x: The pristine carbon, BC-0.5, BC-1 and BC-2 samples were dispersed into 125 mL of gold(III) chloride solution, followed by the addition of 12 mL of sodium borohydride solution (molar ratio of Au/$NaBH_4$: 1:2). The as-obtained

Au_y/C, Au_y/BC-0.5, Au_y/BC-1 and Au_y/BC-2 samples (y% represents the contents of Au) were then washed for three times with distilled water.

Catalytic coupling of (1-bromoethyl) benzene: Coupling reactions of (1-bromoethyl) benzene were performed by dispersing 10 mg of catalyst and 1.2 mmol of substrates into 3 mmol of allyltributylstannane liquid. The solution was then reacted at 50 °C for 1h under vigorously stirring. The final product was identified by GC-MS and quantified by GC with an FID detector.

Hot filtration test: After a two-hour reaction, the catalyst was removed by filtration. The remaining filtrate reacted for another four hours.

Recycling reaction: After the reaction, the catalyst was collected by filtration and washed with 1 mL of dichloromethane for three times. Then, the catalyst was used for following reaction.

Cyclic voltammetry (CV) experiment: The CV measurement was conducted via a three-electrode system consisted of a platinum counter electrode and a Ag/AgCl reference electrode. 3 mg of sample was added into 0.8 mL of ethanol to form a homogenous ink under sonication. Then, 0.06 mL of ink was added dropwise onto a F-doped SnO_2 (FTO) transparent substrate electrodes (1x1 cm^2) to use as a working electrode. 0.1M $TEABF_4$ in acetonitrile was used as supporting electrolyte.

Mott-Schottky plots test: The same three-electrode system was used as described above except the electrolyte was changed to 0.5M Na_2SO_4.

Theoretical calculation: Density functional theory (DFT) was used with the DMol3 program to perform the theoretical calculation. The generalized gradient approximation (GGA) method treated by the Perdew-Burke-Ernzerhof (PBE) functional was used to optimize the structures. The double numerical plus polarization (DNP) basis set was used and the DFT semi-core pseudopots method was employed for core treatment. The Au/BC-x catalysts were simulated on graphene sheet (5x5) and the distance of each Au atoms was fixed as 2.884 Å. The concentration of B atom in Au/BC-1 was similar to the result of the ICP test. The adsorption energy (ΔE_{ads}) was calculated as the following equation:

$$\Delta E_{ads} = E_{br\text{-}Au/BC} - E_{br} - E_{Au/BC}$$

Where $E_{br\text{-}Au/BC}$, $E_{Au/BC}$ and E_{br} represent total energy of a (1-bromoethyl) benzene molecule absorbed on the Au/BC-x, Au/BC-x system, and the (1-bromoethyl) benzene molecule respectively.

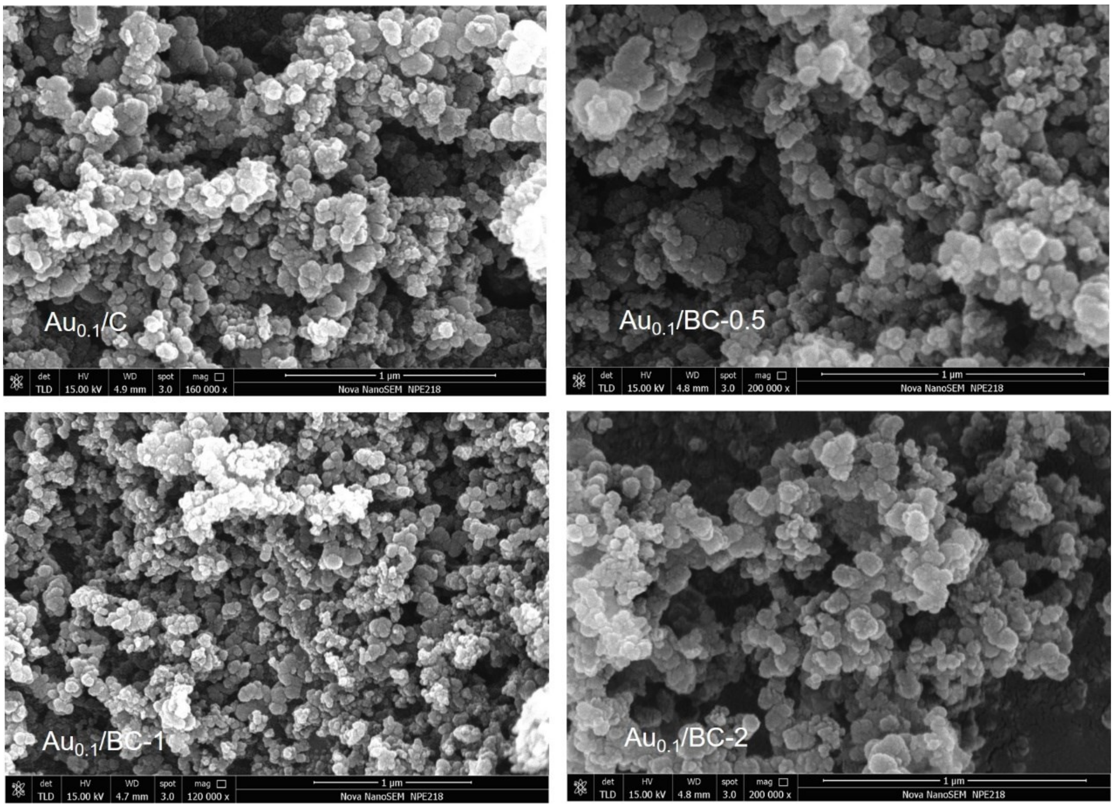

Figure S1. SEM images of Au$_{0.1}$/C, Au$_{0.1}$/BC-0.5, Au$_{0.1}$/BC-1 or Au$_{0.1}$/BC-2 samples. The spherical structures of carbons are well maintained during the thermal condensation process and the deposition of Au nanoparticles.

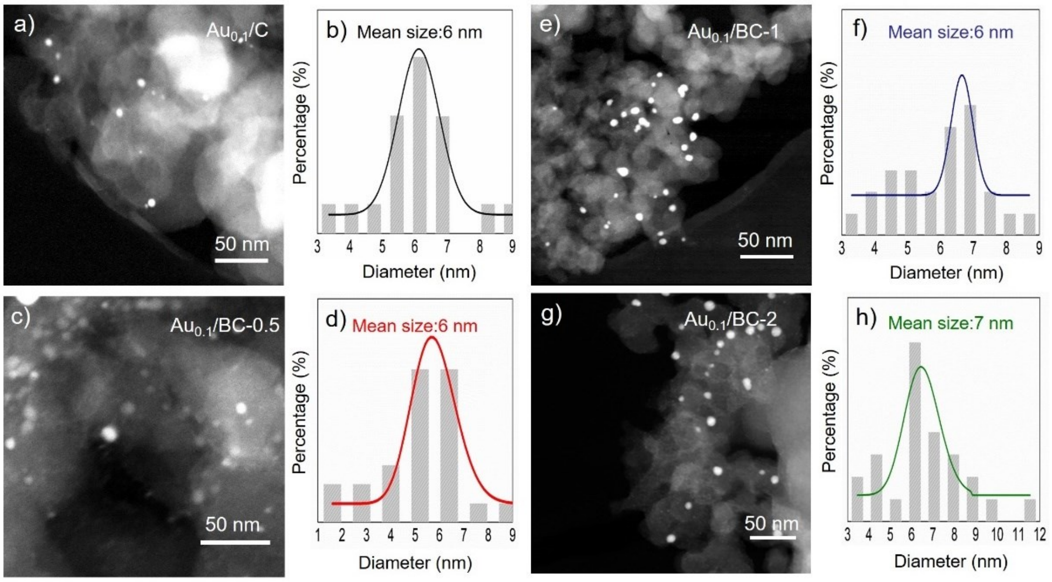

Figure S2. TEM images and size distributions of Au nanoparticles of $Au_{0.1}$/C (a, b), $Au_{0.1}$/BC-0.5 (c, d), $Au_{0.1}$/BC-1 (e, f) or $Au_{0.1}$/BC-2 (g, h) samples. Au particles on different carbon supports have similar mean sizes, excluding the possible size effect of Au components on the final catalytic activity of Au/BC catalysts with varied B dopant concentrations in this work.

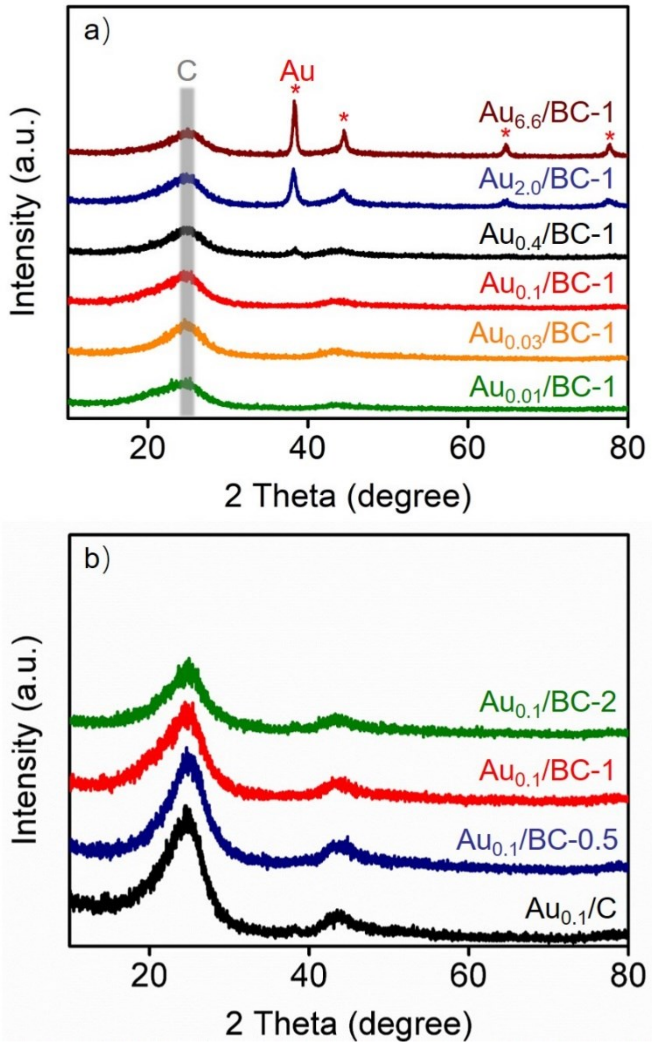

Figure S3. XRD patterns of Au$_y$/BC-x samples. Gradual increased Au typical peaks were observed as more Au species introduced (a). Typical graphite peaks of carbon components become broader as more B dopants introduced, indicating a slight disturb in the graphitization degree (b).

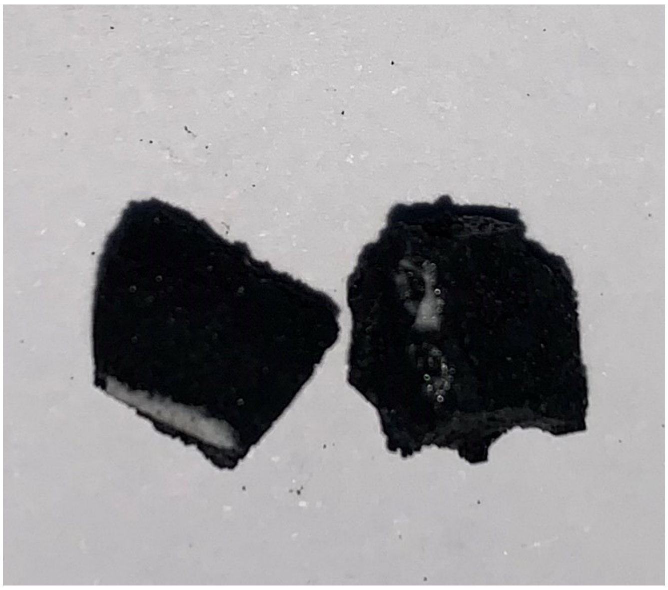

Figure S4. The photograph of the as-obtained BC-2 sample The excess amount of boric acid that are not consumed during the thermal condensation progress.

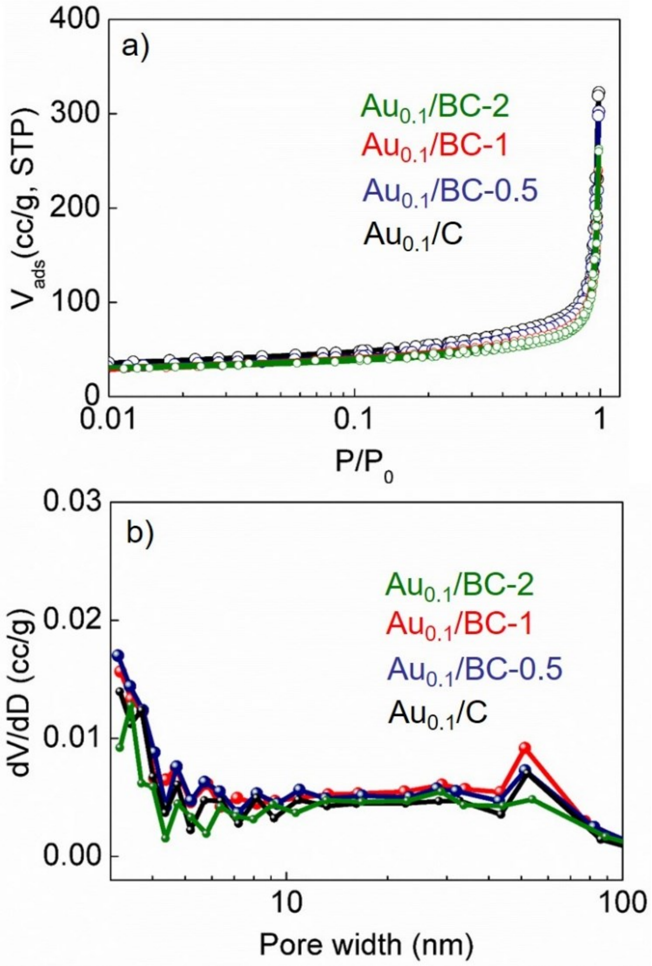

Figure S5. N_2 adsorption/desorption isotherms (a) and pore size distributions (b) of $Au_{0.1}$/C, $Au_{0.1}$/BC-0.5, $Au_{0.1}$/BC-1 or $Au_{0.1}$/BC-2 samples. The comparable pore sizes and BET surface areas exclude the major contribution of surface area of the catalyst surpports to the improved activity of $Au_{0.1}$/BC-x.

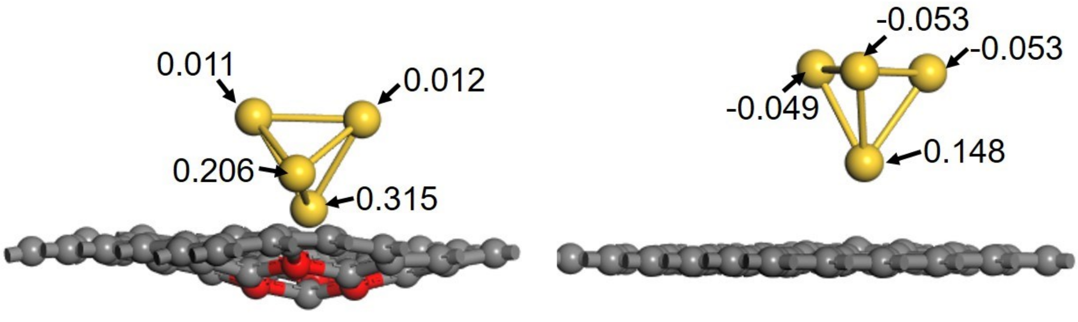

Au/BC-1

Au/C

Figure S6. The calculated Hirshfeld charges of each Au atom on pristine C and BC-1 surface. The BC-1 support attracted 0.544 electrons from the Au cluster (0.14 for each Au atom) while C support gave 0.007 electrons to Au cluster (0.0018 for each Au atom), indicating the formation of electron-deficient Au centres in Au/BC-1 catalyst. (C atom: grey; B atom: red; Au atom: yellow).

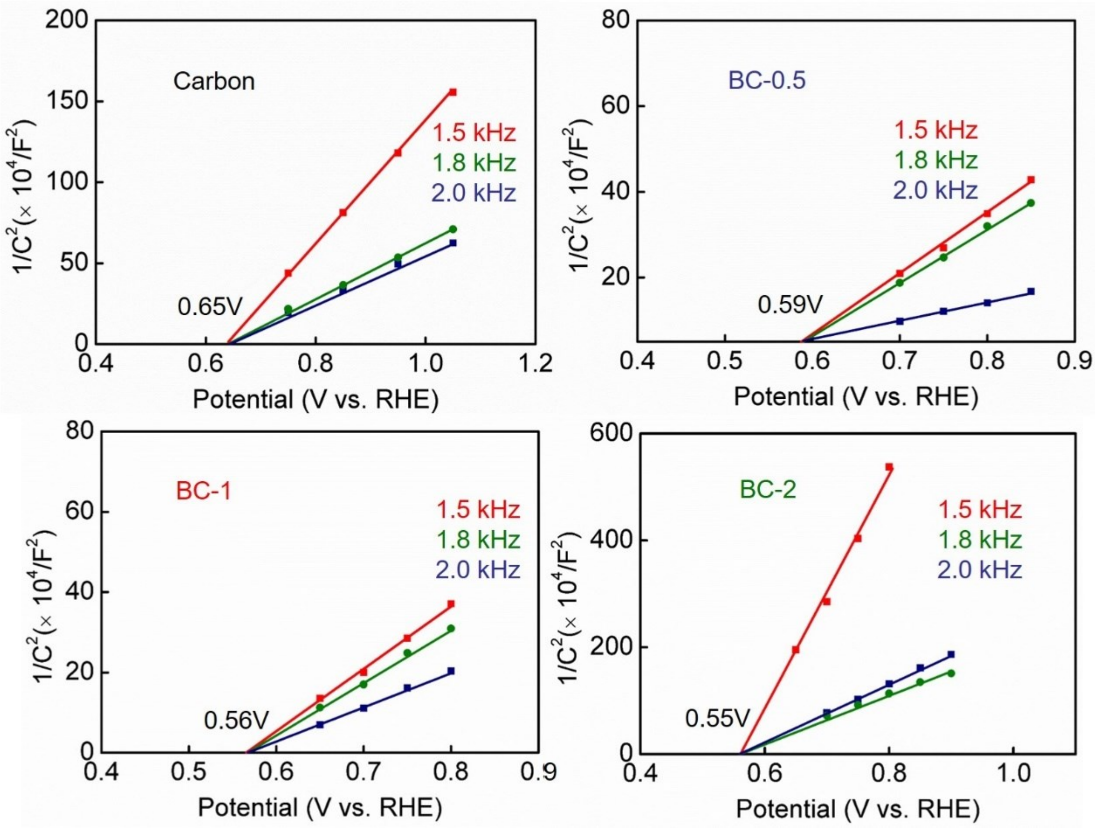

Figure S7. Mott-Schottky plots of pristine carbon, BC-0.5, BC-1 and BC-2 samples at selected frequencies. Increasing the boron contents from 0 to 6% leads to a shift of conduction band position from 0.65 to 0.55 V.

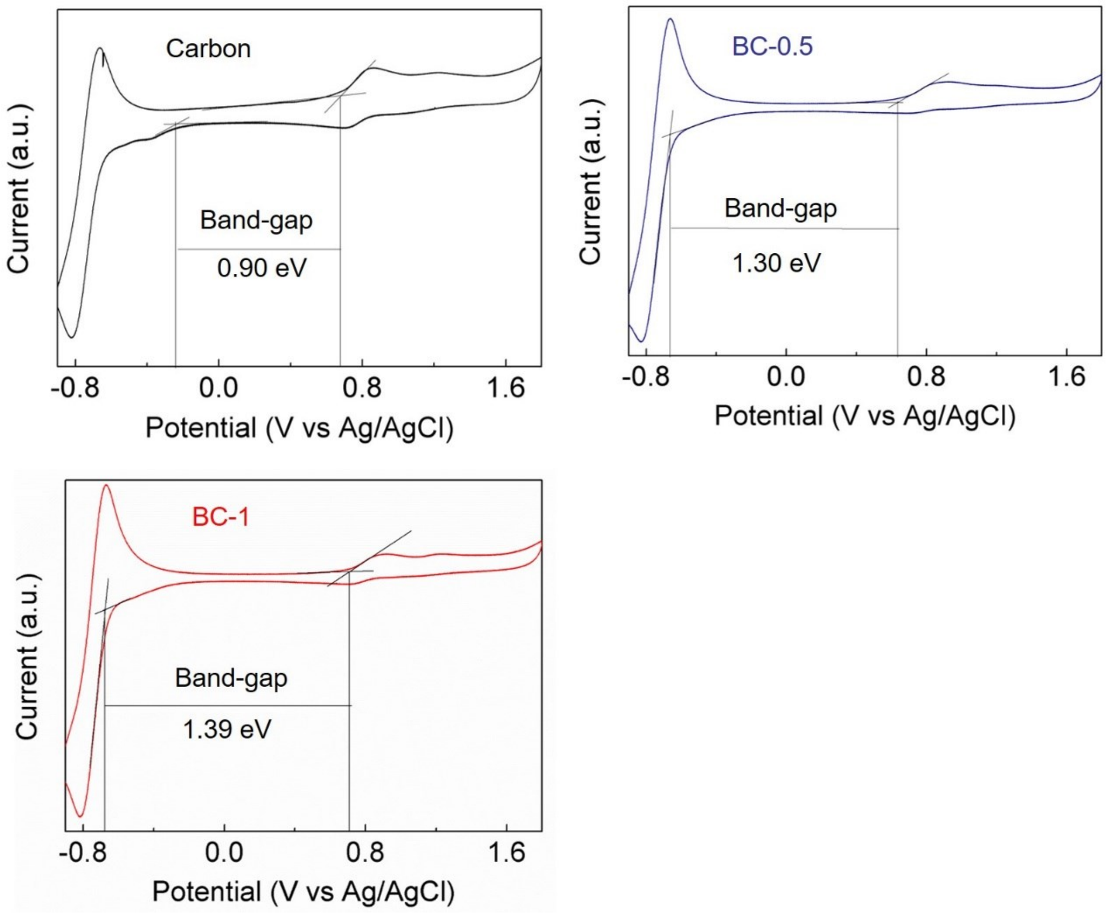

Figure S8. The current-voltage curve for pristine carbon, BC-0.5 and BC-1 samples. The introduced boron heteroatoms opened the band gap of carbon supports.[S1]

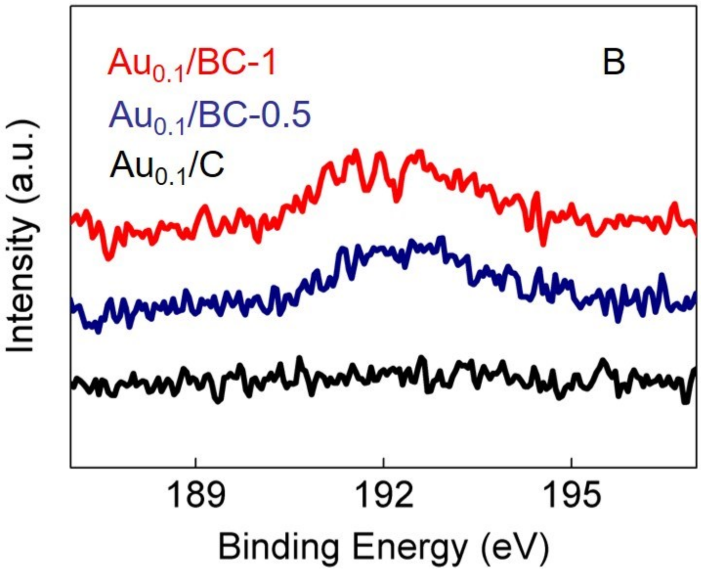

Figure S9. B 1s XPS spectra of $Au_{0.1}$/C, $Au_{0.1}$/BC-0.5 and $Au_{0.1}$/BC-1 samples. Except for $Au_{0.1}$/C, the other catalysts show B 1s peaks at a similar location, indicating the successful introduction of B dopant.

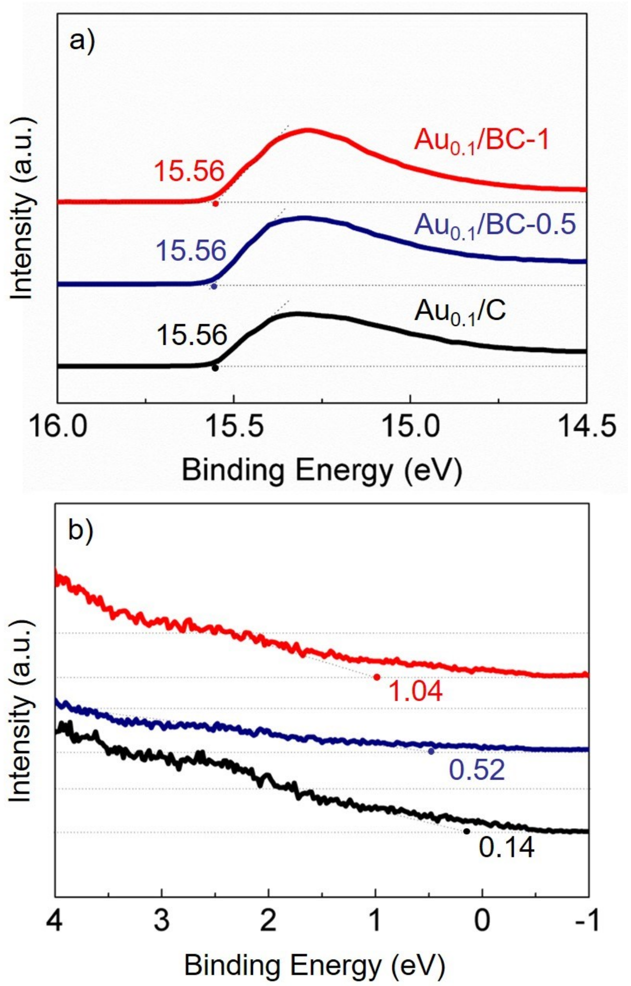

Figure S10. UPS spectra of Au$_{0.1}$/C, Au$_{0.1}$/BC-0.5 and Au$_{0.1}$/BC-1 samples at the cutoff (E$_{cutoff}$) energy (a) and the onset (E$_i$) energy (b) regions. The work function (Φ) of metallic compounds equal to the ionization energy values which can be calculated by $\Phi = 21.21\ \text{eV} - (E_{cutoff} - E_i)$. The work functions of Au$_{0.1}$/C, Au$_{0.1}$/BC-0.5 and Au$_{0.1}$/BC-1 are 5.79, 6.17 and 6.69 eV, respectively.

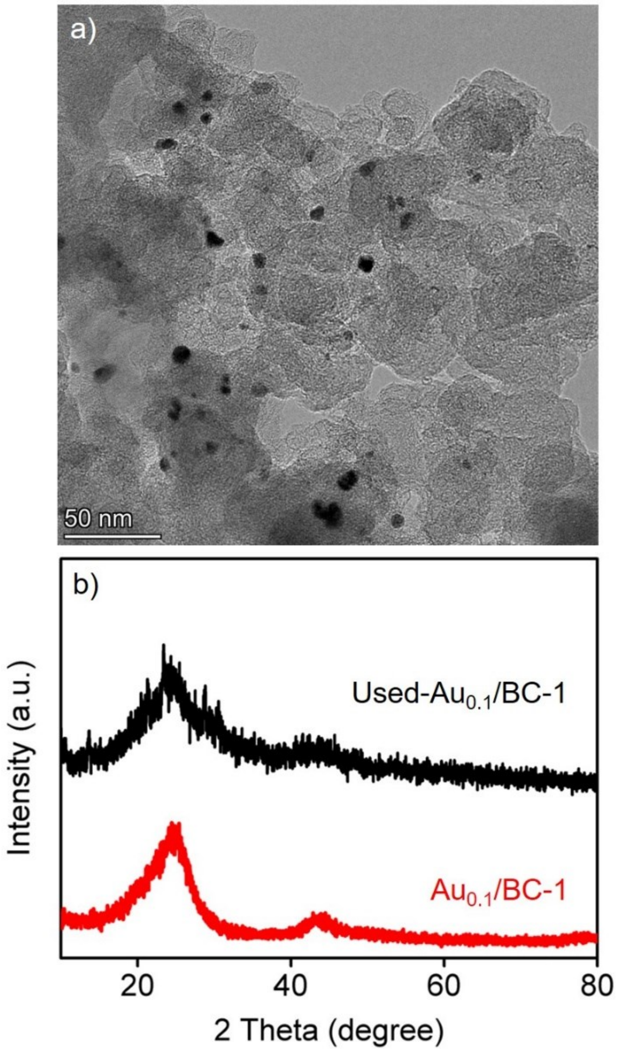

Figure S11. The TEM (a) and XRD (b) image of the Au$_{0.1}$/BC-1 sample after use. Particle size of the Au nanoparticles and the structure of the carbon support were not changed obviously after use in catalytic reactions.

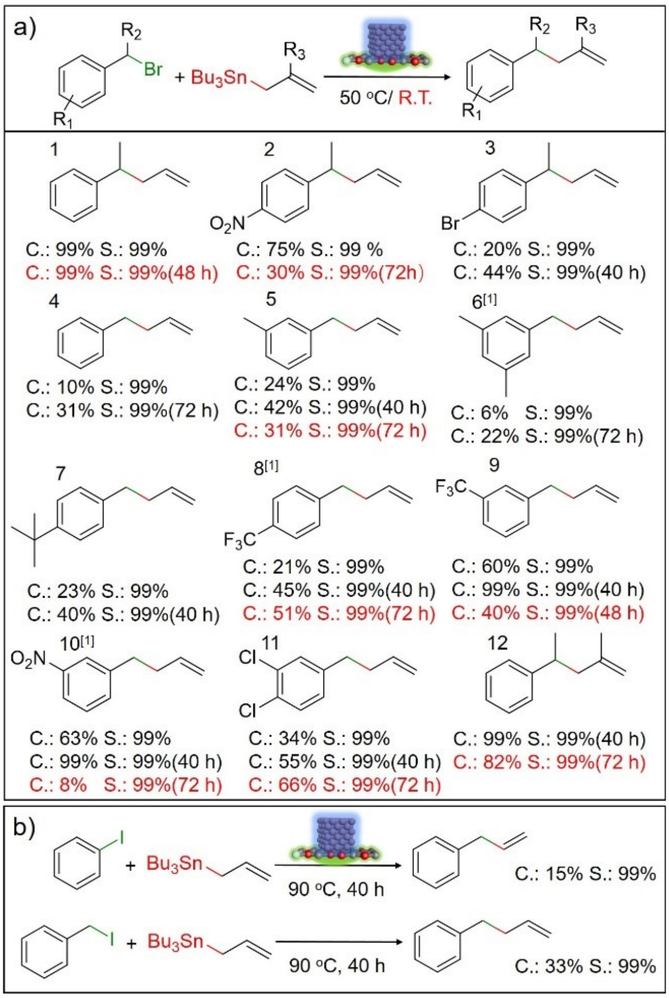

Figure S12. Scope of electron-deficient Au nanoparticles in the Au/BC-1 catalyst. Reaction conditions: 1.2 mmol of substituted benzylic bromides (iodide), 3 mmol of allylstannanes, 3 mg of catalyst at 50 °C (black) or room temperature (red), 20 h, solvent-free. [1] One millilitre of dichloromethane was used as the solvent. To evaluate the scope of the Au/BC-1 catalyst, different substituted benzylic bromides were tested under standard conditions (Figure S11) and at room temperature (highlighted in red in Figure S11). Both the *meta*- and *para*-substituents show comparable conversions and high selectivity. The reactions can be further extended to primary benzylic bromides (Substrates 4-11 in Figure S11) with electron-withdrawing (-CF_3, -Cl, -NO_2) or electron-donating (-CH_3) functional groups, resulting in good conversions (22-99%) and high selectivity (99%). Methallyltri-n-butyltin (Substrate 12 in Figure S11) could also be used as an active coupling partner, achieving complete conversion of 99% with a selectivity of 99%. All these results highlight the good chemical tolerance of the Au/BC-1 catalyst for Stille coupling of substituted benzylic bromides and allylstannanes. It should be noted that (iodomethyl)benzene and iodobenzene could only react with allyltributylstannane at temperatures higher than 90 °C (Figure S11b).

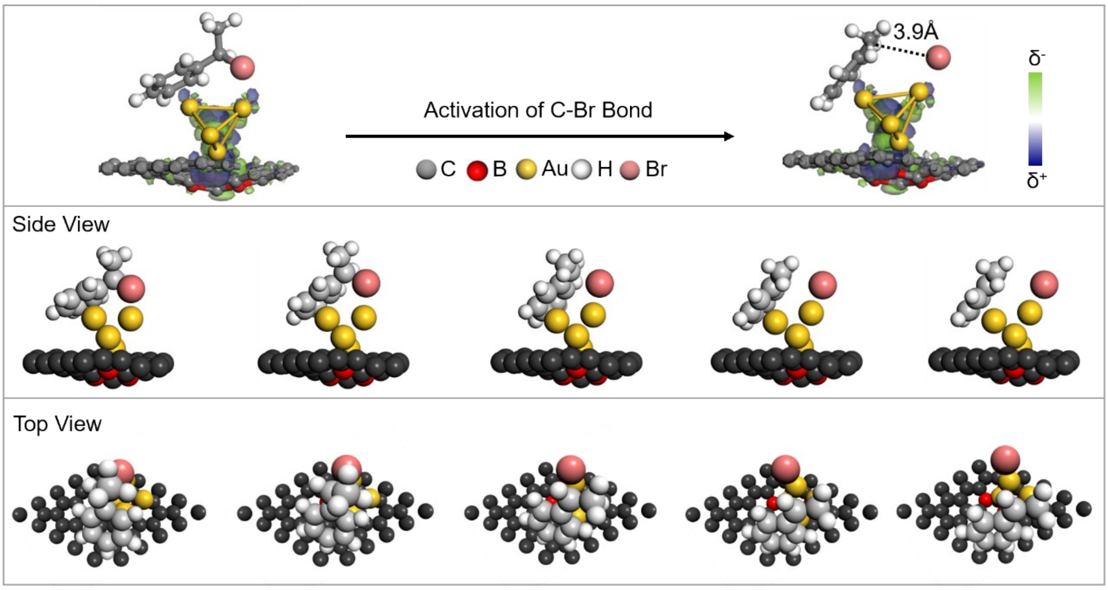

Figure S13. The calculated configurations of (1-bromoethyl) benzene on the Au/BC-1 model during the activation of C-Br bond. An automatic cleavage of C-Br bonds happened when adsorbed on Au/BC-1 catalyst, further confirming the key role of electron-deficient Au nanoparticles in activating the C-Br bond. Such an automatic cleavage process of C-Br bond is also presented in Supplementary Video 1 (top view) and Video 2 (side view).[S2]

Figure S14. The homocoupling reaction catalysed by Au$_{0.1}$/BC-1. Reaction conditions: 1.2 mmol of (bromomethylene)dibenzene, 3 mmol of allyltributylstannane, 3 mg of catalyst, one millilitre of dichloromethane was used as the solvent.

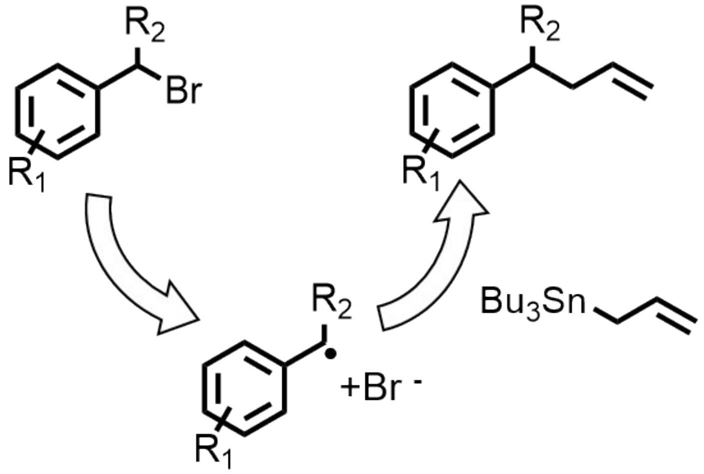

Figure S15. The catalytic mechanism over Au/BC-1. Automatic cleavage of C-Br bonds result in the formation of a benzylic radical and a Br atom adsorbed on the electron-deficient Au surface, further promoting the coupling with allyltributylstannane.

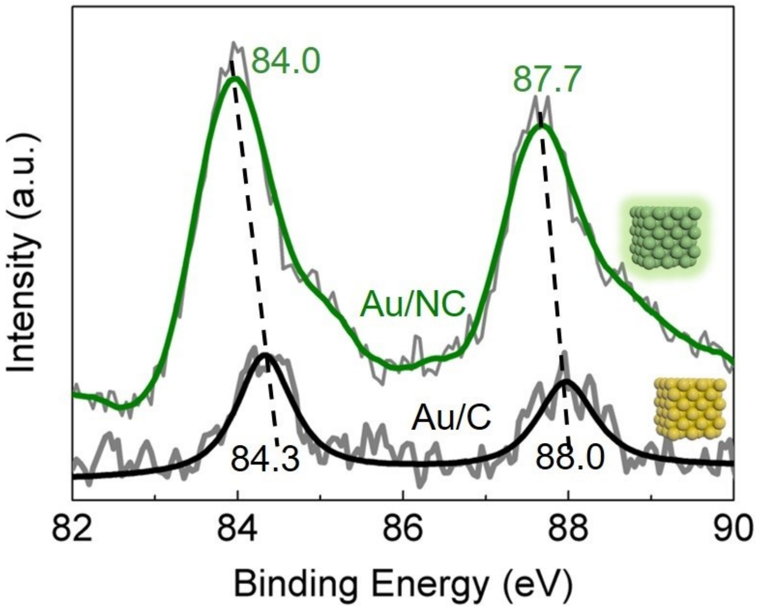

Figure S16. The Au 4f XPS spectra of Au/C and Au/NC catalysts. The Au XPS peaks (84.3 eV and 88.0 eV) shifted to lower binding energy (84.0 eV and 87.7 eV) when carbon support was doped with more nitrogen atoms, indicating the formation of electron-rich Au nanoparticles (green areas) in Au/NC catalyst.

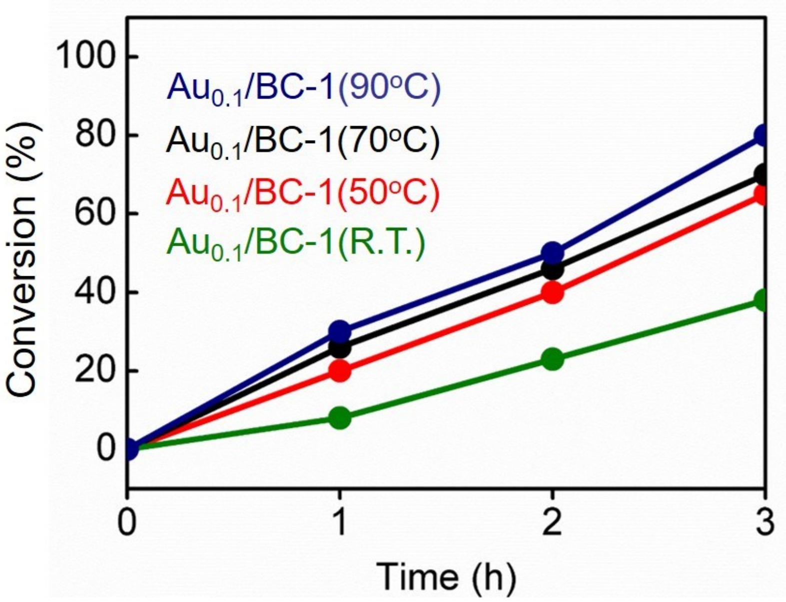

Figure S17. Conversions of (1-bromoethyl) benzene over typical $Au_{0.1}$/BC-1 catalyst at different reaction time and different temperatures. The conversions of (1-bromoethyl) benzene slightly increased with the reaction temperatures, indicating the activation of C-Br bonds over electron-deficient Au nanoparticles makes the coupling reaction less dependent on temperature. Reaction conditions: 1.2 mmol of (1-bromoethyl) benzene, 3 mmol of allyltributylstannane, 10 mg of $Au_{0.1}$/BC-1.

Table S1. The element content of different samples.

Sample	1st round B (wt.%) by ICP	2st round B (wt.%) by ICP	Au (wt.%) by ICP	C (at.%) by XPS	O (at.%) by XPS
$Au_{0.1}$/C	-	-	0.08	96.0	3.2
$Au_{0.1}$/BC-0.5	3.2	3.2	0.07	96.8	2.4
$Au_{0.1}$/BC-1	6.0	6.0	0.06	96.1	2.9
$Au_{0.1}$/BC-2	6.0	6.0	0.06	98.3	1.7

Table S2. The porous structure information.

Sample	Surface area [m^2g^{-1}]	Pore volume [cc g^{-1}]
$Au_{0.1}$/C	185	0.50
$Au_{0.1}$/BC-0.5	189	0.50
$Au_{0.1}$/BC-1	193	0.51
$Au_{0.1}$/BC-2	143	0.41

Table S3. The catalytic activity of different catalysts[a].

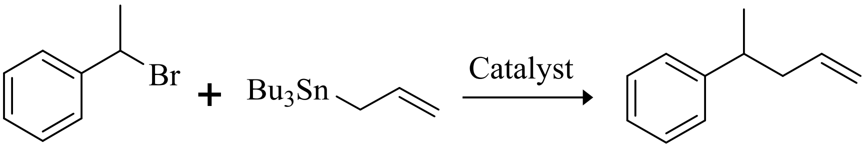

Entry	Catalyst	Time (h)	Conv. (%)	Sel. (%)
1	$Au_{0.1}$/BC-1	0	0	>99
2	$Au_{0.1}$/BC-1	1	20	>99
3	$Au_{0.1}$/BC-1	2	40	>99
4	$Au_{0.1}$/BC-1	4	71	>99
5	$Au_{0.1}$/BC-1	6	99	>99
6	$Au_{0.1}$/C	0	0	>99
7	$Au_{0.1}$/C	1	6	>99
8	$Au_{0.1}$/C	2	10	>99
9	$Au_{0.1}$/C	4	21	>99
10	$Au_{0.1}$/C	6	33	>99
11	BC-1	0	0	>99
12	BC-1	1	0	>99
13	BC-1	2	0	>99
14	BC-1	4	0	>99
15	BC-1	6	0	>99

[a]Reaction conditions: 1.2 mmol of (1-bromoethyl) benzene, 3 mmol of allyltributylstannane, 10 mg of catalyst, 50 ºC.

Table S4. The cycling stability of $Au_{0.1}$/BC-1[a].

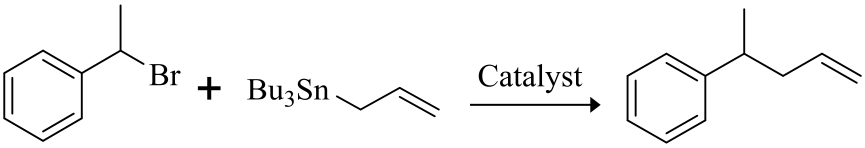

Entry	Catalyst	Cycle Number	Conv. (%)	Sel. (%)
1	$Au_{0.1}$/BC-1	1	81	>99
2	$Au_{0.1}$/BC-1	2	79	>99
3	$Au_{0.1}$/BC-1	3	78	>99
4	$Au_{0.1}$/BC-1	4	76	>99
5	$Au_{0.1}$/BC-1	5	74	>99

[a]Reaction conditions: 1.2 mmol of (1-bromoethyl) benzene, 3 mmol of allyltributylstannane, 10 mg of $Au_{0.1}$/BC-1, 50 ºC, 5h.

Table S5. The catalytic activity of Au_y/BC-1with different Au contents[a].

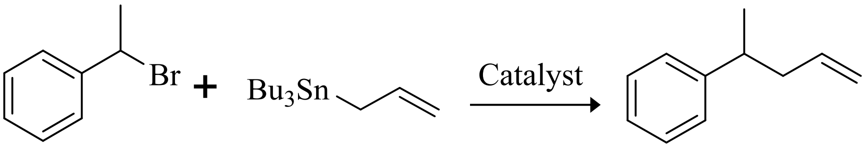

Entry	Catalyst	Conv. (%)	Sel. (%)	TOF (h^{-1})
1	$Au_{0.01}$/BC-1	0.8	>99	5306
2	$Au_{0.03}$/BC-1	3	>99	7880
3	$Au_{0.1}$/BC-1	8	>99	10506
4	$Au_{0.4}$/BC-1	23	>99	4531
5	$Au_{2.0}$/BC-1	41	>99	1615
6	$Au_{6.6}$/BC-1	57	>99	681

[a]Reaction conditions: 1.2 mmol of (1-bromoethyl) benzene, 3 mmol of allyltributylstannane, 3 mg of catalyst, 50 ºC, 1h.

TOF value = (Conversion mol of (1-bromoethyl) benzene)/(Total mol metal)/(Reaction time)

(Conversion mol of (1-bromoethyl) benzene) = (Initial mol of (1-bromoethyl) benzene)) × (Conversion of (1-bromoethyl) benzene))

(Total mol metal) = (Weight of catalyst) × (Mass concentration of Au)/ (Molar mass of Au)

Table S6. The catalytic activity of Au catalysts with different electron density[a].

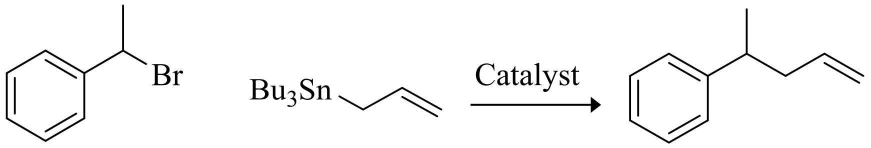

Entry	Catalyst	Conv. (%)	Au contents (wt.%)	Sel. (%)	TOF (h^{-1})
1	$Au_{0.1}$/C	5.6	0.08	>99	4549
2	$Au_{0.1}$/BC-0.5	10.8	0.07	>99	10026
3	$Au_{0.1}$/BC-1	13.6	0.06	>99	14729
4	$Au_{0.1}$/NC	1.6	0.10	>99	1040

[a]Reaction conditions: 47.5 mmol of (1-bromoethyl) benzene, 57 mmol of allyltributylstannane, 12 mg of catalyst, 50 ºC, 12h. (Au contents were determined by ICP results.)

Table S7. The optimization of catalyst/substrate ratios.

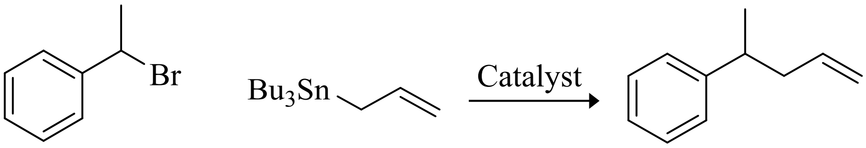

Entry	Catalyst	Time (h)	Scale (mmol)	Conv. (%)	Sel. (%)	TOF (h^{-1})
1[a]	$Au_{0.1}$/BC-1 (3 mg)	1	1.2	8.0	>99	10506
2[a]	$Au_{0.1}$/BC-1 (12 mg)	12	47.5	13.6	>99	14729
3[a]	$Au_{0.1}$/BC-1 (12 mg)	12	95	8.0	>99	17329
4[a]	$Au_{0.1}$/BC-1 (12 mg)	24	120	4.1	>99	5609
5[b]	$Au_{0.1}$/BC-1 (3 mg)	2	1.2	6.0	>99	3940
6[b]	$Au_{0.1}$/BC-1 (12 mg)	12	47.5	4.8	>99	5199
7[b]	$Au_{0.1}$/BC-1 (12 mg)	24	95	1.2	>99	1300
8[b]	$Au_{0.1}$/C (3 mg)	2	1.2	trace	>99	--

[a] 50 °C. [b] Room temperature.

---

4. References

(S1). J. Liu, W. Yang, Y. Li, L. Fan and Y. Li, *Phys. Chem. Chem. Phys.,* 2014**, 16**, 4778-4788.

(S2). C. K. Acharya and C. H. Turner, *J. Phys. Chem. C,* 2007, **111**, 14804-14812.